

Model tests on bearing capacity and accumulated settlement of a single pile in simulated soft rock under axial cyclic loading

Benjiao Zhang, Can Mei, Bin Huang, Xudong Fu*, Gang Luo and Bu Lv

School of Civil Engineering, Wuhan University, No. 16 Luojiaoshan Road, Wuchang District, China

(Received February 26, 2016, Revised September 20, 2016, Accepted December 02, 2016)

Abstract. The research reported herein is concerned with the model testing of piles socketed in soft rock which was simulated by cement, plaster, sand, water and concrete hardening accelerator. Model tests on a single pile socketed in simulated soft rock under axial cyclic loading were conducted and the bearing capacity and accumulated deformation characteristics under different static, and cyclic loads were studied by using a device which combined oneself-designed test apparatus with a dynamic triaxial system. The accumulated deformation of the pile head, and the axial force, were measured by LVDT and strain gauges, respectively. Test results show that the static load ratio (SLR), cyclic load ratio (CLR), and the number of cycles affect the accumulated deformation, cyclic secant modulus of pile head, and ultimate bearing capacity. The accumulated deformation increases with increasing numbers of cycles, however, its rate of growth decreases and is asymptotic to zero. The cyclic secant modulus of pile head increases and then decreases with the growth in the number of cycles, and finally remains stable after 50 cycles. The ultimate bearing capacity of the pile is increased by about 30% because of the cyclic loading thereon, and the axial force is changed due to the applied cyclic shear stress. According to the test results, the development of accumulated settlement is analysed. Finally, an empirical formula for accumulated settlement, considering the effects of the number of cycles, the static load ratio, the cyclic load ratio and the uniaxial compressive strength, is proposed which can be used for feasibility studies or preliminary design of pile foundations on soft rock subjected to cyclic loading.

Keywords: simulated soft rock; model tests; static load ratio; cyclic load ratio; number of cycles; cyclic secant modulus

1. Introduction

Soft rock is broadly distributed: mudstone and shale account for about 50% of the earth's surface rocks, and rock-socketed pile foundations in soft rock have been widely used. Foundation piles are normally and advantageously used for the transfer of loads acting in axial direction in many fields of application. In addition to the static loads, piles are also subjected to earthquakes, operation of machines and hammers, construction operations, quarrying, fast moving traffic, wind, or loading due to wave action of water. Design of pile foundations to resist axial loads is primarily based on the limiting settlement considering the safe operation of the superstructure. Dynamic loading or cyclic loading has great effects on the accumulated settlement and bearing capacity of pile foundations. Cyclic loading is sparsely considered in design or covered by existing

*Corresponding author, Professor, E-mail: xdfu@whu.edu.cn

specifications. So it is of importance to study the effect of cyclic loading on the bearing capacity, stiffness, and accumulated settlement.

Many scholars have investigated the dynamic response of pile foundations subjected to cyclic axial loads (Lee 1993, Dupla and Canou 2003, Li *et al.* 2012). Chan and Hanna (1980) showed that the cyclic response of displacement piles in sand was affected by the number of cycles, their frequency, the mean shaft load, the shaft cyclic load amplitude, the pile depth, the loading history, and the properties of the surrounding sand. Poulos (1981, 1989) conducted small-scale model tests in sand and found that the critical cyclic loading amplitude causing large deformations was 0.7-0.8 under cyclic loading over 1000 cycles. Al-Douri and Poulos (1995) studied the permanent accumulated displacement of a model pile under constant, and variable amplitude, cyclic loading in calcareous sand. Tsuha *et al.* (2012) and Jardine and Standing (2012) studied the settlement characteristics, shear stress, *inter alia*, of model pile under cyclic load in sand: axial cyclic pile responses were categorised as stable, unstable, or meta-stable according to the number of cycles. They reviewed the potential effects of cyclic loading on offshore piles and considered how these may be addressed in practical design. Furthermore, the bearing capacity of a pile would be significantly improved when the amplitude of any cyclic loading was optimised (Le Kouby *et al.* 2004, Jardine *et al.* 2006, D'Aguiar *et al.* 2009). Bekki *et al.* (2013) indicated that the side friction on a pile would show strain hardening because of the phenomenon of shear dilatancy under a large number of cycles. Chen *et al.* (2013) and Ren (2013) studied the cyclic performance of pile foundation subjected to long-term axial cyclic loading in silt by using a large-scale test-rig.

Although many scholars have studied the accumulated settlement and bearing capacity characteristics of pile foundations under cyclic loading, the soils in these tests are mostly soft clay, sand, or silt. The cyclic loading of pile foundations in soft rock is rarely reported.

In view of the above, a test device, combined self-designed test apparatus with a dynamic triaxial test-rig to assess a single pile bearing mechanism, was used to conduct cyclic loading tests on a single model pile socketed in soft rock. The work studied the influence of static load ratio and cyclic load ratio on the accumulated settlement of pile head, the axial force in the pile shaft, the cyclic secant modulus, and its static characteristics.

This paper provides the experimental basis for assessment of the response characteristics of a pile socketed in soft rock under dynamic cyclic loading. And these results can be very useful as a first-hand observation and as a resource for validation of numerical analysis. Based on the tests results, an empirical formula for accumulated settlement is proposed which can be used for feasibility studies or preliminary design of pile foundations on soft rock subjected to cyclic loading.

2. Experiment design

2.1 Test device

Tests of a single model pile bearing characteristics under axial cyclic loading were conducted on a device which combined a test apparatus with a dynamic triaxial test-rig (Fig. 1). The self-designed test apparatus includes the calibration chamber, model piles, the connection and other accessories. The calibration chamber for all the tests in the present experimental work was a steel cylinder having an internal diameter of 320 mm and a height of 540 mm. The connection was designed to connect the model piles and the load cell. As preliminary test indicated that the failure plug formed below the pile base was about 4 times the pile diameter, and the failure formed

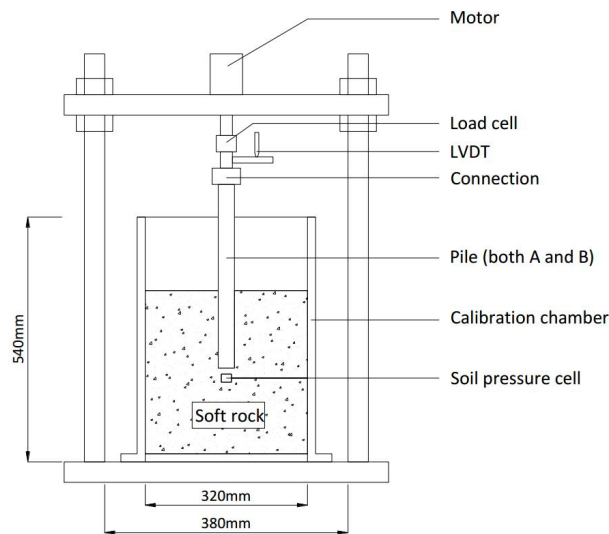


Fig. 1 Test device

around the pile was about 3 times the pile diameter, it was hence decided that as long as the clearance between the pile base and the calibration chamber base exceeded 4 four times the pile diameter, the boundary effect due to container base would be minimal.

2.2 Model piles

The materials that used to manufacture model piles usually are perspex bar, aluminum tube (aluminum bar) and steel tube. Meanwhile, the elastic modulus of them are 3.15 GPa, 70 GPa and 200~210 GPa (Q235), respectively. However, the strain gauges would only be fixed on the outside surface of the perspex bar and may be easily destroyed (Yu 2009). Sometimes the mild steel (low carbon steel) rod has been used to make model piles because of low strength and rigidity (Shanker *et al.* 2007). The strain of aluminum is about 3 times that of the steel when they are subjected to the same loading. The greater strain is beneficial for calculating the axial force of pile shaft. Comparing with two other materials, the aluminum tubing could be more appropriately to simulate the C30 concrete pile, which has an elastic modulus of 30 GPa.

Many scholars have employed the aluminium tubing to simulate model piles since it has an equivalent structural stiffness as that of a solid concrete pile (Boominathan and Ayothiraman 2005, Patra and Pise 2006, Achmus and Thieken 2010, Dykeman and Valsangkar 2011, Ayothiraman and Boominathan 2013). The aluminium used had yield strength of 294 MPa and an elastic modulus of 70 GPa.

Model piles in this paper include model pile A and model pile B. Model pile A was made of aluminium tube with an outer diameter of 40 mm and wall thickness of 3 mm. Length to diameter ratio (L/d) of pile A was 20. Ten pairs of strain gauges were fixed on the internal surface thereof. Fig. 2 shows the strain gauges arrangement and model piles. The dimensions of the substrates are 10 mm × 3 mm and their resistance is 120Ω. The strain gauges were covered with epoxy AB glue after being stuck by 502 glue. The epoxy AB glue is moisture-proof, an insulator, and, as such, protects the strain gauges. Another aluminium pipe with the same properties of model pile A was

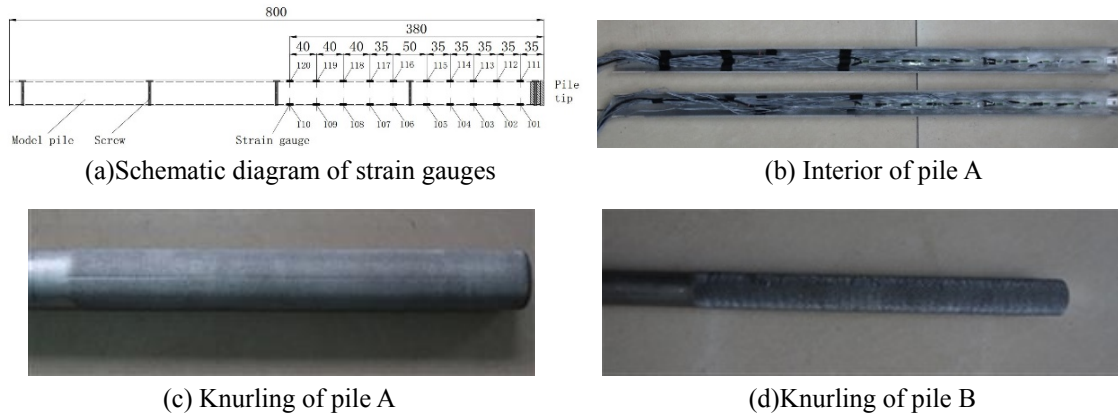


Fig. 2 Strain gauges arrangement and model piles

used as the temperature compensation pile. Twenty strain gauges were fixed on its outside surface. The temperature compensation strain gauges could decrease the errors caused by temperature and humidity change. Meanwhile, model pile B was made of aluminium alloy bar (Type 2A12) with a diameter of 24 mm and a length of 500 mm. However, no strain gauges were fixed on its outside or inside surface of pile B. Both piles were knurled on the surface of the pile tip over a length of 300 mm and to a depth of 0.5 mm. The tubing surface was knurled to simulate a roughened pile surface (Leung *et al.* 1993).

The model pile A and the strain gauges were calibrated before and after testing. The incremental change in every strain gauge showed a linear relationship with applied load ($r^2 > 0.999$).

2.3 Synthetic materials

Synthetic materials can be readily made and reproduced in identical batches in the laboratory, thereby eliminating the costs of excavation and transportation of natural soft rock (Indraratna 1990). In addition, comparison of the simulated soft rock with various rocks, all the mechanical parameters are among the range of different rock types. The simulated soft rock made by synthetic materials has similar physical and mechanical properties to the natural soft rock. So the simulated soft rock is used widely to replace the natural soft rock in the laboratory model experiments. The simulated soft rock in this paper is a mixture of cement, plaster, medium sand, water and concrete hardening accelerator. To get the optimal mix proportions, various mixes were made and subjected to unconfined compressive strength testing on $\phi 50 \text{ mm} \times \text{H}100 \text{ mm}$ specimens. The optimal mix proportions were cement : plaster : medium sand : water : concrete hardening accelerator of 4.5% : 5.0% : 84.71% : 4.75% : 1.04%. The unconfined compressive strength of the simulated soft rock sample is 1.44 MPa and the deformation modulus is 157.88 MPa.

In simple terms, the natural soft rock was formed from the compaction and consolidation of fine-grained marine sediments over many millions of years. This process involved the expulsion of pore water under an increasing weight of overburden to decrease the voids ratio and the development of bonds between the individual particles. The engineering properties of the soft rock are directly related to the saturated water content, stress history and the voids ratio (Johnston and Choi 1986). However, the simulated materials may have a difficulty in simulating the fissures,

joint, structural surfaces, discontinuities and stress history of the actual rocks since they are found to be homogeneous and isotropic. And the small laboratory specimens are also not representative of the actual field behaviour, which is influenced by a much larger scale effect.

2.4 Sample preparation

The model sample was stratified for preparation. To ensure homogeneity, the height of each layer of compacted soil was controlled according to its density. A certain amount of soft rock material substitute was placed into the bottom of the calibration chamber, and the model pile was then installed vertically in the middle of the chamber and fixed with clamps. Finally the soft rock material was filled around the model pile and compacted with a hammer. A regular roughened surface would be formed between the model pile and the simulated soft rock during the compaction since the model pile surface was knurled to simulate a roughened pile surface. The homogeneity of the whole specimen was important. The rock-socketed depth of the model piles was 5 times the pile diameter.

After preparation, the model was covered with a rubber membrane for curing in a constant humidity surroundings for seven days before testing.

During the period of installation in situ, when a pile is driven or jacked into the soils and sand, there is a region around the tip of the pile where extensive disturbance and swelling of the soil takes place (Randolph *et al.* 1979, Bond and Jardine 1991, Randolph 2003). However, the installation of the model piles in laboratory, the simulated soft rock around the piles would not be disturbed. This method can guarantee the homogeneity of the model samples and improve the accuracy of the test results.

2.5 Cyclic loading tests

The frequency of pile foundation cyclic loading tests ranges from 0.002 to 0.1 Hz. According to other test results on bridge and railway pile foundations, most of them are subjected to dynamic load at 0.2 to 3.0 Hz. The frequency used here was 0.2 Hz and the data were sampled at 50 Hz. The effect of frequency on the response characteristics of pile will be analysed in future research. The sinusoidal waveform cyclic load, applied to the model pile head, was servo-controlled and defined as

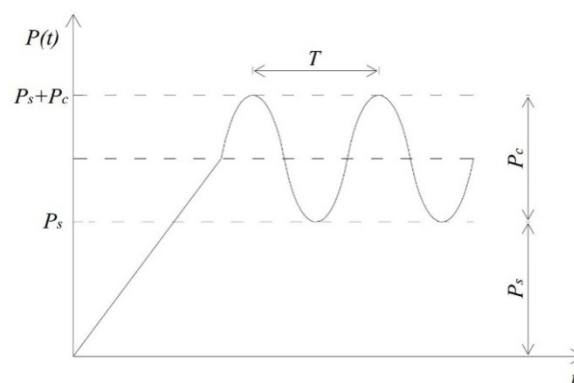


Fig. 3 The cyclic loading regime

Table 1 Cyclic loading test programme

Test no.	Pile diameter (mm)	SLR	CLR	Number of cycles
MP1	24	0.00	0.60	1000
MP2	24	0.10	0.40	1000
MP3	24	0.10	0.60	1000
MP4	24	0.10	0.80	1000
MP5	24	0.20	0.20	1000
MP6	24	0.20	0.40	1000
MP7	24	0.20	0.60	1000
MP8	24	0.30	0.20	1000
MP9	24	0.30	0.40	1000
MP10	40	0.24	0.24	360

$$P(t) = P_s + \frac{1}{2} P_c + \frac{1}{2} P_c \sin(\omega t) \quad (1)$$

where $P(t)$ represents the cyclic loading applied to the model pile head by the actuator; P_s is the static load; P_c is the amplitude of cyclic loading; ω is the circular frequency of cyclic loading, $\omega = 2\pi f$. The cyclic loading is shown in Fig. 3.

As shown in Fig. 3, the static load ratio is defined as $SLR = P_s/P_u$; the cyclic load ratio is defined as $CLR = P_c/P_u$, and P_u is the ultimate bearing capacity.

This work mainly focuses on the dynamic response characteristics of a single pile under one-way compression stress cyclic loading. It should satisfy the following relationship

$$0 \leq CLR + SLR \leq 1 \quad (2)$$

2.6 Test programme

Static loading tests were carried out to ensure the vertical ultimate bearing capacity of the single pile when the strength of simulated soft rock reached stabilisation. Then the cyclic loading tests were conducted under different SLRs and CLR. After that, the static loading tests were carried out again to identify the influence of cyclic loading on the static bearing capacity. The SLR and CLR are considered here at a frequency of 0.2 Hz. The testing programme is summarised in Table 1.

The static loading tests used quick maintenance loading, as recommended by ASTM (1994), and the failure criterion of the pile foundation was a sharp increasing settlement in pile head. For dynamic loading tests, the tests were stopped when they met one of two criteria: (1) the number of cycles reached 1000; or (2) the occurrence of a sharp increasing settlement in pile head.

3. Analysis of test results

3.1 Accumulated settlement of pile head

Under vertical cyclic loading, the soft rock under the pile tip was subjected to cyclic

compressive stress meanwhile the pile-rock interface was subjected to repeated shear stress. Cyclic loading led to a certain amount of accumulated settlement which was the macro-behavioural manifestation of residual plastic deformation of the simulated soft rock. Fig. 4 shows the load-displacement curve of model pile B at $SLR = 0.30$ and $CLR = 0.40$. Fig. 5(a) shows the accumulated displacement-number of cycles (N) curves under different CLR s at $SLR = 0.10$. Meanwhile, Fig. 5(b) shows the accumulated displacement- N curves under different SLR s at $CLR = 0.60$.

From Figs. 5(a)-(b), the accumulated displacement of the pile head was related to SLR , CLR , N , and the uniaxial compressive strength (q_u) of the soft rock. That is

$$\Delta s(N) = f(SLR, CLR, N, q_u) \tag{3}$$

The displacement decreases with increasing of q_u . However, the displacement increases with increasing of SLR , CLR , and N .

To understand better the increase of accumulated displacement, the accumulated settlement results were normalised. The non-dimensional settlement of the pile was proposed, and it can be

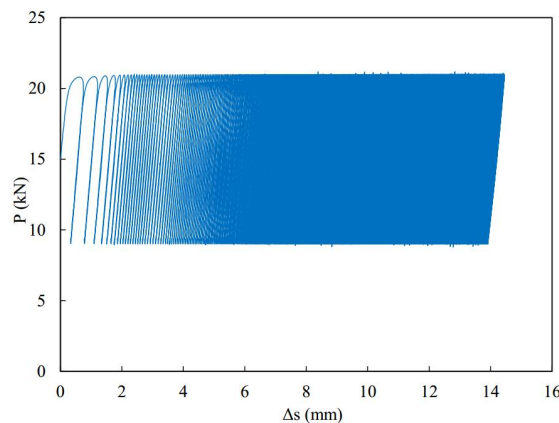


Fig. 4 Cyclic load-displacement curve of model pile B ($SLR = 0.30$, $CLR = 0.40$)

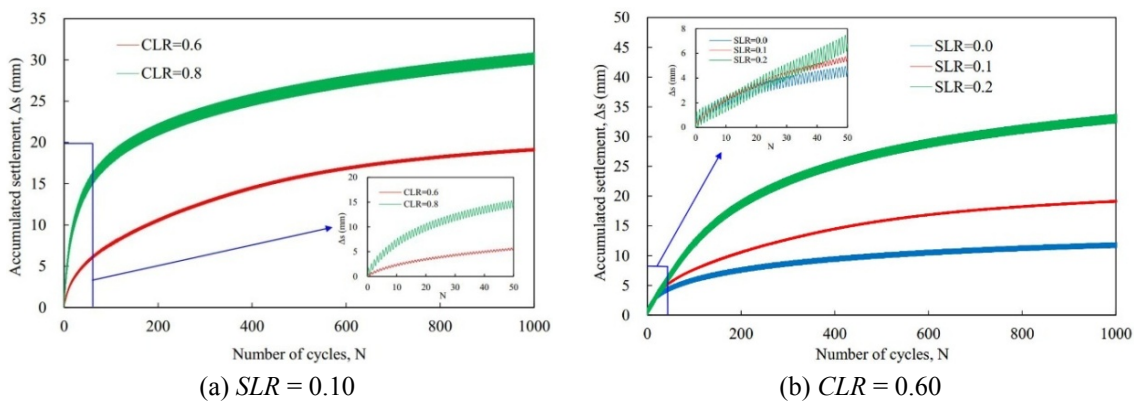


Fig. 5 Development of accumulated displacement during dynamic loading tests

used to predict the accumulated settlement of the pile in laboratory tests. The non-dimensional settlement of the pile head under N load cycles can be expressed as

$$\frac{\Delta s(N)}{S_s} = \frac{S_N - S_0}{S_s} \tag{4}$$

where S_N is the maximum settlement of the pile head under N load cycles; S_0 is the deformation without cyclic loading; S_s is the displacement at the same load, given by $((SLR + CLR) \times Q_u)$ under static load. Thence, the accumulated displacements are plotted in double logarithmic coordinates (Fig. 6).

Fig. 6 shows that the relationship between non-dimensional accumulated settlement and number of cycles can be matched by a power function, that is, it shows a linear relationship in log-log coordinates. So the accumulated settlement under cyclic loading can be expressed as

$$\frac{\Delta s(N)}{S_s} = \frac{1}{q_u^k} AN^b \tag{5}$$

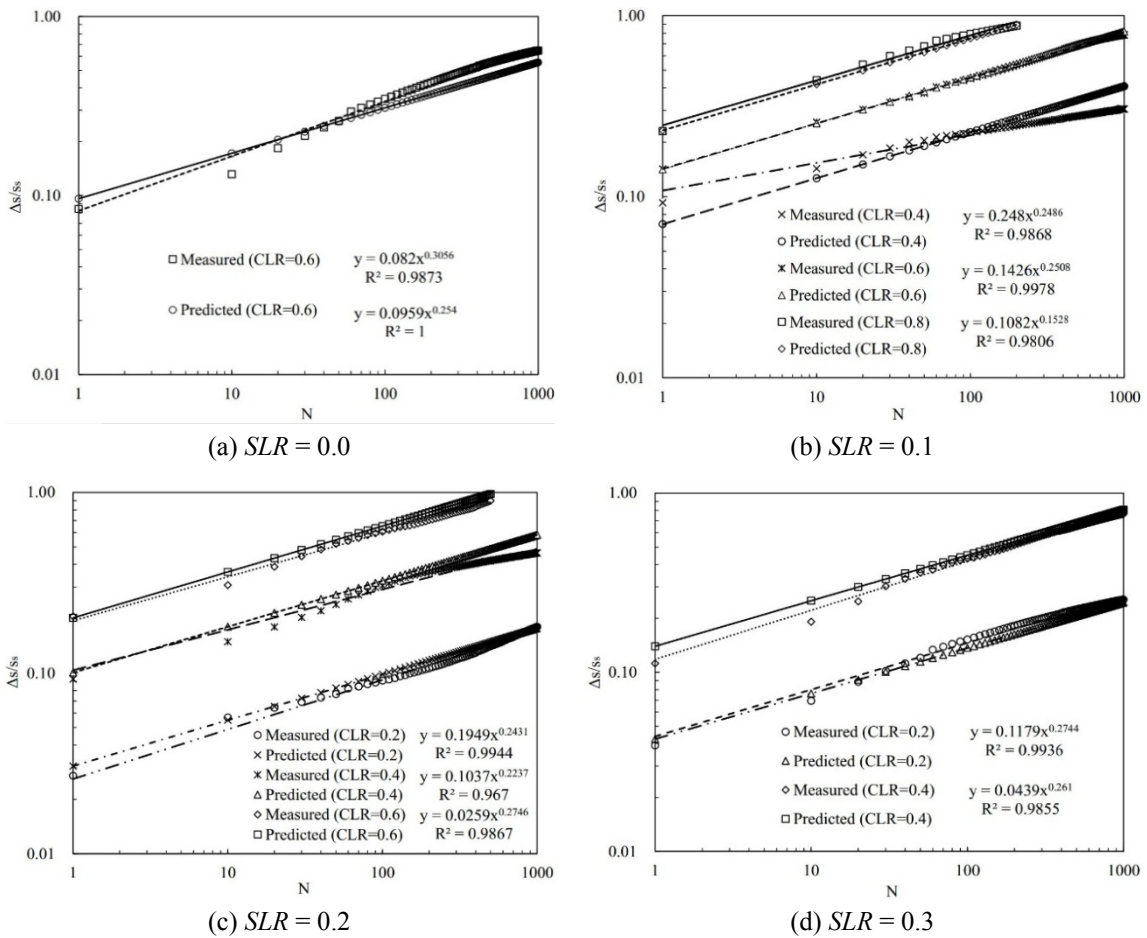


Fig. 6 Variation of non-dimensional accumulated displacement during dynamic load tests

Table 2 Back-analysis results: model parameters for accumulated displacement

Parameter	a	b	m	n
Value	0.231	4.090	1.720	0.254

where A and b are best-fit parameters. The slopes of the accumulated settlement curves are similar, so b is regarded as a constant. The effect of cyclic loading on parameter A is given by Eq. (6)

$$A = a(SLR + 1)^m (CLR)^n \tag{6}$$

where a , m and n are model parameters. When $CLR = 0$, $A = 0$: this means that there is no cyclic accumulated settlement under static loading. When $SLR = 0$, $A = a(CLR)^n$. The accumulated settlement is mainly determined by CLR .

From Eqs. (5)-(6), it follows that

$$\frac{\Delta s(N)}{S_s} = \frac{1}{q_u^k} a(SLR + 1)^m (CLR)^n N^b \tag{7}$$

where q_u is the uniaxial compressive strength (1.44 MPa here), and k is the influence coefficient (taken as 1 here).

To obtain the value of the aforementioned model parameters, Eq. (7) was used to match the results in Fig. 6. The model parameters obtained by back-analysis are summarised in Table 2.

Substituting model parameters q_u and k into Eq. (7), the final prediction of the accumulated settlement of the pile head under cyclic loading tests is

$$\frac{\Delta s(N)}{S_s} = 0.16(SLR + 1)^{4.09} (CLR)^{1.72} N^{0.254} \tag{8}$$

As seen from Fig. 6, the theoretical calculations and experimental results are consistent and the model can incorporate the effect of cyclic loading on accumulated settlement.

The proposed computational model can predict the tests results at $q_u = 1.44$ MPa and $k = 1$. The value of k should be further verified if the model is to be extended to other strengths of soft rock.

3.2 Cyclic secant modulus

Fig. 7 shows the load-settlement hysteresis loops of a model pile. It can be seen that, with the generation of residual deformation, load-settlement hysteresis loops are not closed, while with increasing of numbers of cycles, residual deformation gradually stabilises and the hysteresis loops also tend to close (Huang *et al.* 2015). A hysteresis loop includes four stages: loading phase AB with respect to the initial static compression state; unloading phase BC after peak load; unloading phase CD with respect to the initial static compression state; and loading phase DE after the minimum load. Residual deformation mainly occurs in phase AB. The secant modulus of the load-settlement curve should be calculated without using residual deformation data. Fig. 8 shows the non-closed load-settlement hysteresis loops and Fig. 9 shows the variation of cyclic secant modulus under different CLR.

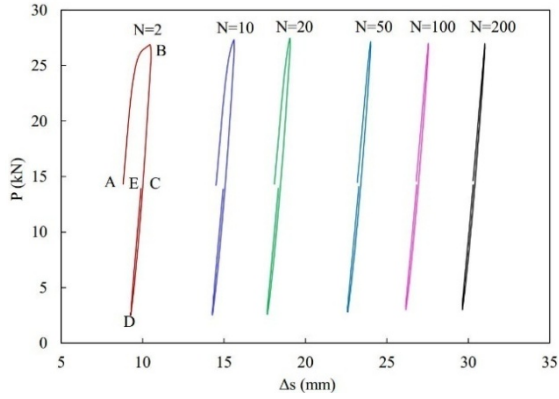


Fig. 7 Load-settlement hysteresis loops for various values of N

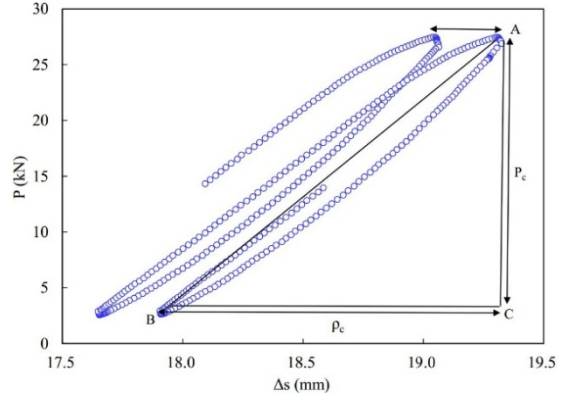


Fig. 8 Non-closed load-settlement hysteresis loops

As seen in Figs. 7 and 8, the cyclic secant modulus of the settlement curve can be expressed by

$$M_{s,c} = \frac{P_c}{\rho_c} (MN/m) \tag{9}$$

where P_c is the full amplitude of the cyclic load; ρ_c is the amplitude of the dynamic settlement which is the difference between the settlement at point A and the settlement at point B in a single cycle.

Fig. 9 shows that the cyclic secant modulus ($M_{s,c}$) firstly increases, then decreases, and finally tends to a stable value as N increasing. The value of $M_{s,c}$ reaches its peak at $6 \leq N \leq 8$ while $M_{s,c}$ reaches a stable value at $N \approx 50$ cycles. The secant modulus increased rapidly because the soft rock was compressed and then the secant modulus began to decrease and eventually reached to a constant value as the soft rock became damaged. The secant modulus decreases marginally and its stable value is about 85% to 95% of its maximum value. The final stable secant modulus is still higher (by about 30%) than that of the initial stiffness. The soft rock particles would be damaged

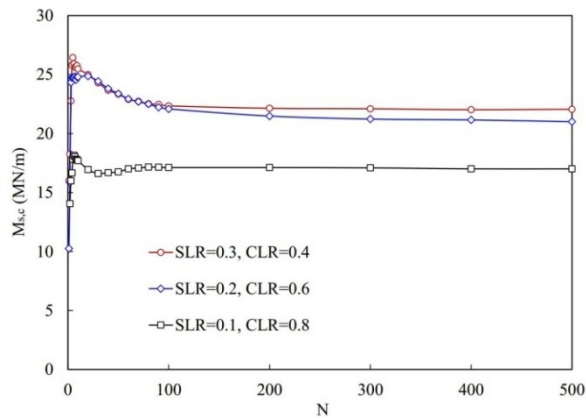


Fig. 9 Variation of cyclic secant modulus for different CLR values

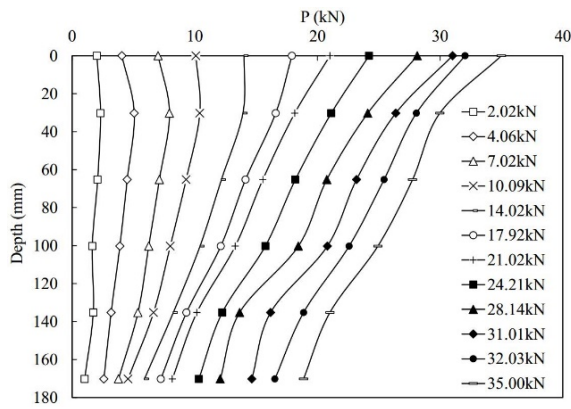


Fig. 10 Typical distribution of axial force along the pile during static loading tests

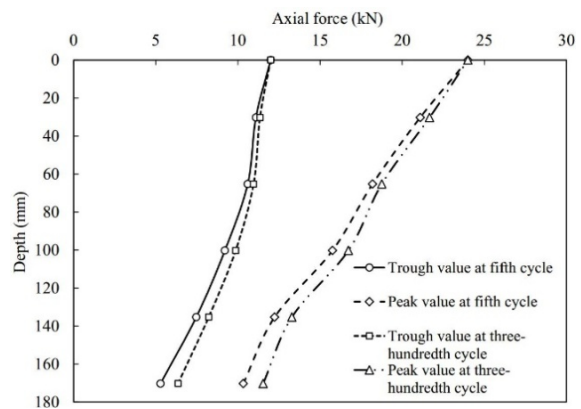


Fig. 11 Variation of axial force under dynamic load

more seriously and the cyclic secant modulus gradually decreases with the increasing of CLR. Here, the cyclic secant modulus is between 10.25 and 26.43 MN/m.

3.3 Axial force on the pile

Fig. 10 shows the distribution of axial force on model pile A under static load. It indicates the development of axial force from pile head to pile tip under all levels of load. Under multi-stage loading, the rate of decay of axial force gradually changed: the axial force was less attenuated since the pile tip resistance and shaft friction acted synchronously when the load was small; the decay rate of the axial force increased because of the development of skin friction when the load increased. However, the desired ultimate displacement to mobilise full shaft friction was much smaller than that required to mobilise the full extent of the tip resistance. So when the pile load increased, this increasing load was borne by the pile tip. The decay rate of the axial force was unchanged in this case.

The distribution of pile axial force changed because of the effect of cyclic loading. Fig. 11 shows the distribution of axial force in model pile A at the fifth, and three-hundredth, cycle peak and trough values with the combination of dynamic load at $SLR = 0.24$ and $CLR = 0.24$. From the distribution of axial force, when the cyclic loading on the pile head is at rough, that is, only static loading is applied on the pile head, the axial force is a little higher than the initial load (to a certain extent) after 300 cycles. This indicates that dynamic loading would cause a variation of axial force under static loading on a single pile and the pile tip bears much more of the total load. The increasing axial force illustrates that the side friction, provided by the pile-rock interface, diminishes.

3.4 Influence of cyclic load on static characteristics

For micro-piles, graph-plotting is often used to determine the asymptote to predict the ultimate bearing capacity, where the Chin-Kondner hyperbolic model (C-K model) is the most widely used method (Chin 1970, 1972, Fleming 1992, Akgüner and Kirkit 2012). The typical $P-s$ curve of a single pile is shown in Fig. 12.

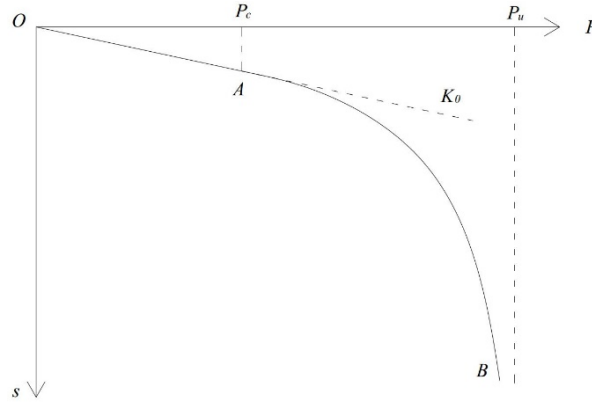


Fig. 12 Typical P - s curve of a single pile under static load

As shown in Fig. 12, the load-settlement curve is non-linear and can be divided into two stages: (1) stage OA, in which the foundation is in an elastic state, where the load P is less than the critical plastic load P_c ; (2) stage AB, in which the foundation is in an elasto-plastic state, where P is between P_c and the ultimate load P_u .

In general, the load on the pile head (P) and the settlement (s) in a static loading test can be approximated by a Chin-Kondner hyperbolic model

$$P = \frac{s}{C_1 \cdot s + C_2} \quad (10)$$

where C_1 and C_2 are constants, which can be determined experimentally. The tangent derivative of any point of this curve is

$$\frac{dP}{ds} = \frac{C_2}{(C_1 \cdot s + C_2)^2} \quad (11)$$

From Eq. (13), as $s \rightarrow \infty$

$$C_1 = \frac{1}{P_u} \quad (12)$$

From Eq. (14), at the initial point of the tests, when $s = 0$, $E_t = E_i$

$$C_2 = \frac{1}{E_i} = \frac{1}{K_0} \quad (13)$$

where E_t and E_i are the tangent modulus and the initial deformation modulus, respectively.

To study the influence of cyclic loading on the static loading characteristics of the pile, static load tests were carried out on the model pile before and after the dynamic loading tests. Fig. 13 shows the load-settlement curves of the static loading tests of model pile B. Test 1 meant that pile B was only subjected to the static loading. Test 2 and Test 3 indicated that pile B was applied static loading again after dynamic loading tests of MP5 and MP2 (Table 1), respectively. Meanwhile, the

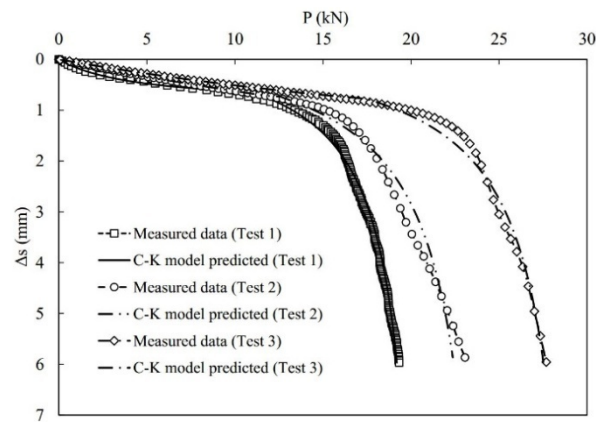


Fig. 13 Load-settlement curves of the static loading tests of model pile B

Table 3 Ultimate bearing capacity of a single pile under different CLR and SLRs

Test no.	SLR	CLR	C_1	C_2	P_u/kN	
					C-K model	Test value
Test 2	0.2	0.2	0.0397	0.0293	25.19	18.71
Test 3	0.1	0.4	0.0332	0.0187	30.12	24.34

ultimate bearing capacity of model pile B was calculated by using of the aforementioned Chin-Kondner hyperbolic model. The parameters C_1 and C_2 , and the test results (ultimate bearing capacity) are summarised in Table 3.

As shown in Fig. 13 and Table 3, the Chin-Kondner hyperbolic model can predict the ultimate bearing capacity of a pile foundation. However, the calculated value, when using the model, is a little bigger than the experimental value because the calculated value is obtained when the settlement (s) tends to infinity (an impossibility in laboratory testing). The load at the inflection point of the load-settlement curves is taken as the ultimate bearing capacity of the pile foundation in these laboratory tests.

The ultimate bearing capacity, and cyclic secant modulus, of a single pile increased after cyclic loading: the greater the CLR, the greater the increase, within a reasonable range. The maximum ultimate bearing capacity of the pile could be increased by about 30%. This shows that the cyclic compressive stress can lead to soft rock particles at the pile tip becoming denser. This also matches the fact that the cyclic secant modulus increases with the increasing number of loads cycles applied.

Although the axial bearing capacity of piles increases under cyclic loading, its application in practical design and in-place is limited by the pile head displacement behaviour under dynamic loading. The pile capacities that are currently being used in the practical design may need to be verified for the effect of cyclic loading on permissible displacement.

4. Conclusions

Through the analysis of the response of a single pile socketed in soft rock under cyclic loading,

the following conclusions can be obtained:

The device combined one self-designed test apparatus with a dynamic triaxial system under axial cyclic loading is significant, which needs to be accounted for in the practical design.

CLR and *SLR* affect the accumulated settlement. The accumulated settlement increases with the increasing of *CLR* and *SLR*. However, the ratio of accumulated settlement at each loading cycle decreases gradually with the increasing number of loading cycles. The relationship between non-dimensional accumulated settlement of the pile head, and the number of cycles, can be represented by a power function, that is, it shows a linear relationship when the data are plotted in log-log coordinates. A computational model of the accumulated settlement of the pile head is proposed which can be used for feasibility studies, or the preliminary design, of pile foundations on soft rock subjected to traffic, or other, cyclic loading.

The cyclic secant modulus firstly increases, then decreases, and finally tends to a stable value with increasing numbers of cycles. The modulus reaches a peak at $6 \leq N \leq 8$ while the modulus reaches a stable value at $N \approx 50$. Meanwhile, the stable value is about 85% to 95% of its maximum value. The final stable secant modulus is still higher (by about 30%) than its initial value.

Dynamic loading causes are ductility in shaft friction, which changes the distribution of axial force in the pile. And the change in axial force mainly occurs at the onset of dynamic loading. The axial force becomes stable with an increasing of number of cycles.

Cyclic loading affects the ultimate bearing capacity of the pile. Within a reasonable range, the ultimate bearing capacity would be improved with the increasing of *CLR* and *SLR* and the maximum improvement of bearing capacity is about 30%.

It should be pointed out that the above conclusions are arrived at based on 1-g model tests conducted in the laboratory. Owing to the fact that the behaviour of piles in soft rock is stress-dependent, which is not simulated realistically in 1-g model tests, the above conclusions may need to be verified as and when full-scale/centrifuge test data under cyclic loading are made available.

The influence of scale effect and the roughened surface on the test results will continue to be studied in future.

Acknowledgments

The authors acknowledge the support from the National Natural Science Foundation of China (Grant Nos.51378403 and 51309028).

References

- Achmus, M. and Thieken, K. (2010), "On the behavior of piles in non-cohesive soil under combined horizontal and vertical loading", *Acta Geotech.*, **5**(3), 199-210.
- Akguner, C. and Kirkit, M. (2012), "Axial bearing capacity of socketed single cast-in-place piles", *Soils Found.*, **52**(1), 59-68.
- Al-Douri, R.H. and Poulos, H.G. (1995), "Predicted and observed cyclic performance of piles in calcareous sand", *J. Geotech. Eng.*, **121**(1), 1-16.
- A.S.T.M. D1143-81 (1994), Standard test method for piles under static axial compressive load, USA.
- Ayothiraman, R. and Boominathan, A. (2013), "Depth of fixity of piles in clay under dynamic lateral load", *Geotech. Geol. Eng.*, **31**(2), 447-461.
- Bekki, H., Canou, J., Tali, B., Dupla, J.C. and Bouafia, A. (2013), "Evolution of local friction along a model

- pile shaft in a calibration chamber for a large number of loading cycles”, *Comptes Rendus Mécanique*, **341**(6), 499-507.
- Bond, A.J. and Jardine, R.J. (1991), “Effects of installing displacement piles in a high OCR clay”, *Géotechnique*, **41**(3), 341-363.
- Boominathan, A. and Ayothiraman, R. (2005), “Dynamic behaviour of laterally loaded model piles in clay”, *Geotech. Eng. J.*, **158**(4), 207-215.
- Chan, S.F. and Hanna, T.H. (1980), “Repeated loading on single piles in sand”, *J. Geotech. Eng. Div.*, **106**(2), 171-188.
- Chen, R.P., Ren, Y., Zhu, B. and Chen, Y.M. (2013), “Deformation behaviour of single pile in silt under long-term cyclic axial loading”, *Proceedings of the 18th International Conference on Soil Mechanics and Geotechnical Engineering*, Paris, France, September.
- Chin, F.K. (1970), “Estimation of the ultimate load of piles not carried to failure”, *Proceedings of the 2nd Southeast Asian Conference on Soil Engineering*, Singapore, June.
- Chin, F.K. (1972), “The inverse slope as a prediction of ultimate bearing capacity of piles”, *Proceedings of the 3rd Southeast Asian Conference on Soil Engineering*, Hong Kong, China, November.
- D’Aguiar, S.C., Caballero, F.L. and Razavi, A.M.F. (2009), “Piles under cyclic loading: study of the friction fatigue and its importance in piles behaviour”, *Proceedings of the 17th International Conference on Soil Mechanics and Geotechnical Engineering*, Alexandria, Egypt, October.
- Dupla, J.C. and Canou, J. (2003), “Cyclic pressuremeter loading and liquefaction properties of sands”, *Soils Found.*, **43**(2), 17-31.
- Dykeman, P. and Valsangkar, A.J. (2011), “Model studies of socketed caissons in soft rock”, *Can. Geotech. J.*, **33**(5), 747-759.
- Fleming, W.G.K. (1992), “A new method for single pile settlement prediction and analysis”, *Géotechnique*, **42**(3), 411-425.
- Huang, B., Fu, X.D., Zhang, B.J. and Qiu, Z.F. (2015), “Test technology and normalized characteristics of dynamic elastic modulus and damping ratio”, *Chinese J. Geotech. Eng.*, **37**(4), 659-666.
- Indraratna, B. (1990), “Development and applications of a synthetic material to simulate soft sedimentary rocks”, *Géotechnique*, **40**(2), 189-200.
- Jardine, R.J. and Standing, J.R. (2012), “Field axial cyclic loading experiments on piles driven in sand”, *Soils Found.*, **52**(4), 723-736.
- Jardine, R.J., Standing, J.R. and Chow, F.C. (2006), “Some observations of the effects of time on the capacity of piles driven in sand”, *Géotechnique*, **56**(4), 227-244.
- Johnston, I.W. and Choi, S.K. (1986), “A synthetic soft rock for laboratory model studies”, *Géotechnique*, **36**(2), 251-263.
- Lee, C.Y. (1993), “Cyclic response of axially loaded pile groups”, *J. Geotech. Eng.*, **119**(9), 1399-1413.
- Le Kouby, A., Chnou, J. and Dupla, J.C. (2004), “Behaviour of model piles subjected to cyclic axial loading”, *Cyclic Behaviour of Soils and Liquefaction Phenomena*, 159-166.
- Leung, C.F. and Ko, H.Y. (1993), “Centrifuge model study of piles socketed in soft rock”, *Soils Found.*, **33**(3), 80-91.
- Li, Z., Bolton, M.D. and Haigh, S.K. (2012), “Cyclic axial behaviour of piles and pile groups in sand”, *Can. Geotech. J.*, **49**(9), 1074-1087.
- Patra, N.R. and Pise, P.J. (2006), “Model pile groups under oblique pullout loads—An investigation”, *Geotech. Geol. Eng.*, **24**, 265-282.
- Poulos, H.G. (1981), “Cyclic axial response of single pile”, *J. Geotech. Geoenviron. Eng.*, **107**(1), 41-58.
- Poulos, H.G. (1989), “Cyclic axial loading analysis of piles in sand”, *J. Geotech. Eng.*, **115**(6), 836-852.
- Randolph, M.F. (2003), “Science and empiricism in pile foundation design”, *Géotechnique*, **53**(10), 847-875.
- Randolph, M.F., Carter, J.P. and Wroth, C.P. (1979), “Driven piles in clay—the effects of installation and subsequent consolidation”, *Géotechnique*, **29**(4), 361-393.
- Ren, Y. (2013), “Model test and theoretical study on deformation behaviour of single piles to long-term cyclic axial loading”, Ph.D. Dissertation; Zhejiang University, Hangzhou, China.
- Shanker, K., Basudhar, P. and Patra, N.R. (2007), “Uplift capacity of single piles: predictions and

- performance”, *Geotech. Geol. Eng.*, **25**(2), 151-161.
- Tsaha, C.H.C., Foray, P.Y., Jardine, R.J., Yang, Z.X., Silva, M. and Rimoy, S. (2012), “Behaviour of displacement piles in sand under cyclic axial loading”, *Soils Found.*, **52**(3), 393-410.
- Yu, Q.Q. (2009), “Test research on characteristic of vertical bearing capacity of super pile group”, Ph.D. Dissertation; Southeast University, Nanjing, China.

CC